

Control of Plasma Dynamics within Double-Gate-Turn-Off Thyristors (D-GTO)

U. Wiesner, R. Sittig

Institut für Elektrophysik, Technische Universität Braunschweig
Hans-Sommer-Str. 66, D-38106 Braunschweig, Germany

Abstract

High voltage GTO's require a subtle control of excess charge to exhibit low forward voltage drop as well as low turn-off loss. In this paper it is investigated whether and to what degree device behaviour could be improved if plasma dynamics is controlled with gate electrodes on cathode and anode side. Computer simulations reveal that such D-GTO's exhibit excellent static characteristics and that with a continuous control of electron to hole current ratios on both sides a reduction of turn-off energy by a factor of about 50 seems possible.

1. Introduction

At present GTO's are widely used in traction applications. But there still exists the desire to improve their performance. To reach this goal several authors investigated the characteristics which are achieved by applying IC-technology. The resulting IGBT's, MCT's and similar devices offer the advantage of considerably reduced expenses for turn-on and turn-off. On-state characteristics and switching behaviour of high voltage devices, however, depend mainly on plasma dynamics within the wide base layer. In this paper, therefore, the ultimate characteristics are investigated that could be obtained if both emitters of a GTO are completely controlled.

Following this idea the decisive compromise for switching devices [1], between high carrier concentration for low forward voltage drop and low storage charge for safe switch-off at low loss, can be avoided and charge carrier lifetime can be chosen as high as possible. Thus at turn-on and during the on-state the D-GTO may be considered as a thyristor without any emitter shorts and a base width of about one carrier diffusion length. During the turn-off phase the complete control of electron- and hole-current densities on both sides allows to firstly deplete the base at a moderate voltage increase and secondly the device is definitely switched-off. At the blocking-state finally the high carrier lifetime ensures a low leakage current.

2. Device structure and static characteristics

2D-calculations were carried out using the device simulator ATLAS [2]. The assumed circuit consists of a voltage source $V_0 = 3200\text{ V}$, an ohmic load $R_L = 80\ \Omega$ and an inductive load $L_L = 400\ \mu\text{H}$ clamped to the voltage of the source by a free wheeling diode. For the interaction with these components a total device area of 1 cm^2 is taken into account. The structure of a segment of the investigated device is sketched in Fig. 1a. With a base doping concentration of $2.5 \cdot 10^{13}\text{ cm}^{-3}$ it exhibits a blocking capability of 4500 V . An effective high-injection carrier lifetime of $\tau_{\text{eff}} = 200\ \mu\text{s}$ is assumed in the wide base layer.

The emitter control is simulated by applying the desired ratio of anode to n-gate current and cathode to p-gate current on the corresponding sides. It has to be emphasized that the following results concern only the structure given in Fig. 1a. For comparison with complete devices the voltage drop across the means for control and the corresponding losses have to be taken into account.

At 300 K a leakage current of $0.5\ \mu\text{A/cm}^2$ at an applied blocking voltage of 3200 V is obtained and the forward voltage drop amounts to only 1.0 V at 40 A/cm^2 .

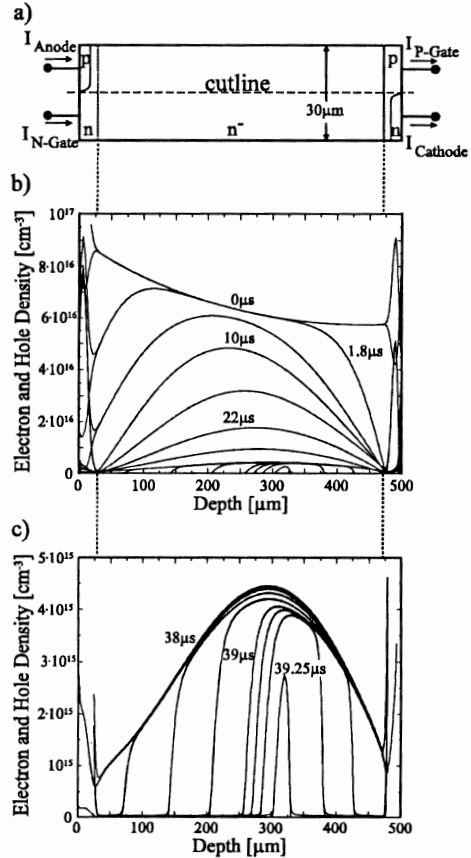


Fig. 1: a) Structure of a segment of the investigated D-GTO. Charge carrier concentration during turn-off along the cutline: b) Complete process, c) Last phase only at an enlarged scale.

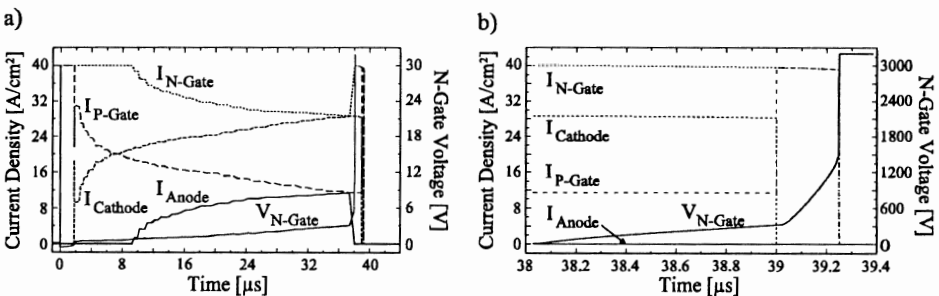


Fig. 2: Emitter and gate currents at turn-off. $V_{N\text{-Gate}}$ represents the n-gate potential when cathode or p-gate contact is grounded: a) Complete process, b) Final emitter switch-off at a spread time scale.

3. Turn-off control

As depicted in Fig. 1b the average carrier concentration in the base amounts to approximately $7 \cdot 10^{16} \text{ cm}^{-3}$ during the on-state ($0 \mu\text{s}$). For depletion in a first step both emitters are switched-off resulting in a pure electron current density at the anode via n-gate and a pure hole current density at the cathode side via p-gate. There the corresponding carrier concentrations drop to about $1 \cdot 10^{15} \text{ cm}^{-3}$. They have to be maintained at this level to avoid build-up of a space charge layer and a corresponding voltage increase. Therefore again rising emitter currents have to be admitted after $1.8 \mu\text{s}$ at the cathode and after $9.5 \mu\text{s}$ at the anode. These emitter current densities, however, do not add up to the applied total current density. Due to the concentration gradients carriers are removed via both gate electrodes. Finally after $38 \mu\text{s}$ the average carrier concentration is reduced to less than $3 \cdot 10^{15} \text{ cm}^{-3}$, while the voltage drop still amounts to less than 4 V.

For final switch-off a delay between turn-off of anode emitter and cathode emitter can be chosen to minimize turn-off loss and to control the position of the residual stored carriers. As soon as the anode emitter is switched-off, at $t = 38 \mu\text{s}$, holes are removed from this side and the current there is maintained by electrons being supplied from the residual reservoir. This leads to a negative space charge, an electric field peak at the nn^- -junction and a corresponding increase of voltage. When at $t = 39 \mu\text{s}$ the cathode emitter is switched-off too, the pn -junction becomes depleted and the space charge layer extends into the carrier reservoir from the cathode side. Only $0.25 \mu\text{s}$ later all carriers are removed and voltage rises sharply up to the clamped voltage. The curves of the corresponding emitter- and gate-currents are shown in Fig. 2 and the actual power loss as well as the integrated turn-off energy are depicted in Fig. 3.

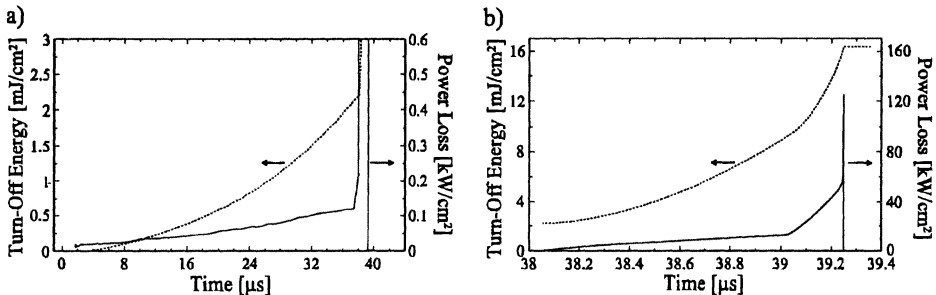


Fig. 3: Actual turn-off loss and integrated energy loss: a) Complete process, b) During the final phase at a spread time scale.

4. Comparison of turn-off losses

Experimental investigations of high voltage D-GTO's revealed already that a considerable reduction of turn-off energy loss can be obtained [3]. In these experiments, however, only delay time between turn-off of anode and cathode emitter was varied. Such a turn-off procedure was simulated, however, on a D-GTO exhibiting a blocking capability of 2000 V. A current density of $40 \text{ A}/\text{cm}^2$ is switched-off against an applied voltage of 1000 V. The resulting turn-off energy versus delay time is sketched in Fig. 4. By choosing a suited delay time energy loss can be reduced in this case by a factor of 9 similar to the value published in [3].

If an optimized turn-off control with a depletion phase as described in section 3 is applied, then loss for the low voltage device could be further reduced by a factor of 6 down to a turn-off energy of 0.75 mJ/cm^2 (marked by the dotted line in Fig. 4). This value can also be compared with turn-off losses reported for high voltage MCT and IGBT [4]. For these devices switched on one side only an energy of 42 mJ/cm^2 was obtained which is just the amount of the D-GTO at zero delay between anode and cathode switch-off.

5. Conclusion

By computer simulations it is confirmed that D-GTO's seem to offer excellent device characteristics for high voltage applications. Since charge carriers can be controlled from both sides a high carrier lifetime can be chosen. This way a low forward voltage drop and a low leakage current in the blocking state are reached. Applying a well adjusted emitter control during turn-off energy loss could be reduced by a factor of 50 compared to devices with one side switching.

The threshold for dynamic avalanche during the steep voltage rise is nearly doubled since electric field builds-up within two different space charge regions. Moreover even if carrier multiplication is triggered it will last only a very short time due to the reduced reservoir and it may be expected that it will not suffice to re-trigger emitter current.

However several further aspects of device behaviour have to be investigated and at present nothing can be said concerning the required expenses for the continuous control of both emitters.

References

- [1] R. Sittig, "Chances, Errors and Progress - A Survey on Power Device Development", Proc. of the Conf. to the 25th anniversary of the Laboratoire d'Analyse et d'Architecture des Systemes, Toulouse, Cèpadues-Editions, Toulouse, pp 159-175, 93
- [2] ATLAS 2D Device Simulation Framework, User's Manual, Silvaco International
- [3] T. Ogura, A. Nakagawa, M. Atsuta, Y. Kamei and K. Takigami, "High-Frequency 6000 V Double-Gate GTO's", IEEE Transactions on Electron Devices, Vol. 40, No. 3, pp 628-633, March 93
- [4] F. Bauer, T. Stockmeier, H. Dettmer, H. Lendenmann and W. Fichtner, "On the Suitability of BiMOS High Power Devices in intelligent, snubberless Power Conditioning Circuits", Proc. of the 6th Internat. Symposium on Power Semiconductor Devices & IC's, Davos, Switzerland, pp 201-206, 94

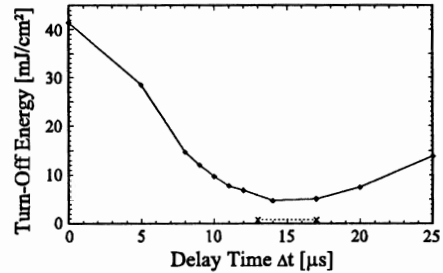


Fig. 4: Turn-off energy of a D-GTO versus delay time between switch-off of anode and cathode emitter., ($I = 40 \text{ A/cm}^2$, $V = 1000 \text{ V}$, $T = 300 \text{ K}$). The dotted line marks the energy loss obtained for optimized emitter control (without relevance to the delay time scale).